J Biomol NMR (2007) 39:177–185
DOI 10.1007/s10858-007-9185-3

ARTICLE

Carbonyl carbon label selective (CCLS) ^{1}H–^{15}N HSQC experiment for improved detection of backbone ^{13}C–^{15}N cross peaks in larger proteins

Marco Tonelli · Larry R. Masterson · Klaas Hallenga · Gianluigi Veglia · John L. Markley

Received: 23 May 2007 / Accepted: 7 August 2007 / Published online: 9 September 2007

Abstract We present a highly sensitive pulse sequence, carbonyl carbon label selective ^{1}H–^{15}N HSQC (CCLS-HSQC) for the detection of signals from ^{1}H–^{15}N units involved in $^{13}C'$–^{15}N linkages. The CCLS-HSQC pulse sequence utilizes a modified ^{15}N CT evolution period equal to $1/(2^{1}J_{NC'})$ (~33 ms) to select for $^{13}C'$–^{15}N pairs. By collecting CCLS-HSQC and HNCO data for two proteins (8 kDa ubiquitin and 20 kDa HscB) at various temperatures (5–40°C) in order to vary correlation times, we demonstrate the superiority of the CCLS-HSQC pulse sequence for proteins with long correlation times (i.e. higher molecular weight). We then show that the CCLS-HSQC experiment yields assignments in the case of a 41 kDa protein incorporating pairs of ^{15}N- and $^{13}C'$-labeled amino acids, where a TROSY 2D-HN(CO) had failed. Although the approach requires that the ^{1}H–^{15}N HSQC cross peaks be observable, it does not require deuteration of the protein. The method is suitable for larger proteins and is less affected by conformational exchange than HNCO experiments, which require a longer period of transverse ^{15}N magnetization. The method also is tolerant to the partial loss of signal from isotopic dilution (scrambling). This approach will be applicable to families of proteins that have been resistant to NMR structural and dynamic analysis, such as large enzymes, and partially folded or unfolded proteins.

Keywords Backbone resonance assignment · Selective labeling · 2D-HNCO · Protein kinase A

M. Tonelli · K. Hallenga · J. L. Markley (✉)
National Magnetic Resonance Facility at Madison,
Department of Biochemistry, University of Wisconsin-Madison,
433 Babcock Drive, Madison, WI 53706, USA
e-mail: markley@nmrfam.wisc.edu

L. R. Masterson · G. Veglia
Departments of Chemistry and Biochemistry,
Molecular Biology, and Biophysics, University of Minnesota,
Minneapolis, MN 55455, USA

Introduction

Recent advances have enabled NMR investigations of proteins as large as 800 kDa (Riek et al. 2002). However, the *conditio sine qua non* for NMR structural, dynamic, and binding studies is the resonance assignment. Sequential assignment strategies rely on multidimensional experiments governed by magnetization transfer through scalar couplings that link spin systems (Clore and Gronenborn 1994). These methods can work for proteins labeled uniformly with ^{15}N and ^{13}C up to about 35 kDa. Larger proteins generally require the use of TROSY (transverse relaxation optimized spectroscopy) based pulse sequences (Pervushin et al. 1997) and perdeuteration combined with selective labeling (Gardner et al. 1998; Tugarinov et al. 2004). However, these methods fall short when conformational exchange (Wagner 1993) or isotopic dilution effects (Lian and Middleton 2001) lead to sensitivity losses and incomplete spectral information (Abdulaev et al. 2006; Tzakos et al. 2006; Vogtherr et al. 2006). A useful approach with larger proteins is to incorporate pairs of ^{15}N- and $^{13}C'$-labeled amino acids and to use one-bond ^{15}N–$^{13}C'$ correlations to assign linked dipeptides (Kainosho and Tsuji 1982; McIntosh and Dahlquist 1990; Tzakos et al. 2006; Yabuki et al. 1998). However, unfavorable dynamics or dilution of the isotopic labels can make these

correlations difficult to detect by conventional NMR methods, such as a 2D-[^{1}H/^{15}N]-TROSY-HN(CO).

We propose here a new method for detecting ^{1}H–^{15}N signals associated with ^{15}N–^{13}C′ backbone pairs. The method utilizes the carbonyl carbon label selective (CCLS) ^{1}H–^{15}N HSQC pulse sequence shown in Fig. 1. It relies on a shorter magnetization transfer period between ^{15}N and ^{13}C′ and is based on the detection of ^{1}H–^{15}N correlations without ^{13}C′ evolution.

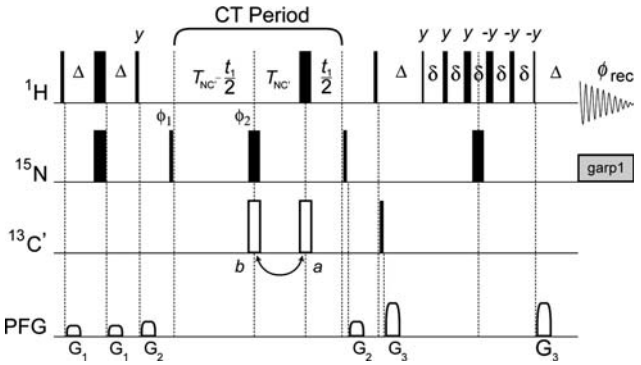

Fig. 1 Schematic of the CCLS-HSQC pulse sequence. The reference spectrum is obtained by executing the pulse sequence with the 180° ^{13}C′ pulse (open rectangle) at position *a*; the ^{13}C′ suppressed spectrum is obtained with this pulse at position *b*. Unless indicated otherwise, all rectangular pulses are applied along the *x*-axis with a flip angle of 90° (narrow bars) or 180° (wide bars). The carrier frequency for ^{1}H is set on resonance with water at 4.77 ppm; the carrier frequency for ^{15}N is set in the center of the amide region at 121.8 ppm; for ^{13}C pulses the offset is set to the C′ region at 174.8 ppm. A 3-9-19 watergate pulse scheme is used in the reverse INEPT transfer to suppress the strong water signal. Garp1 decoupling with a field strength of 1 kHz is used on ^{15}N during acquisition. Delay durations: $\Delta = 2.4$ ms; $\delta = 0.11$ ms; $T_{NC'} = 16.5$ ms. Phase cycling: $\phi_1 = x,-x$, $\phi_2 = x,x,-x,-x$, $\phi_{rec} = x,-x$. To accomplish States quadrature detection for the ^{15}N indirect dimension, a second FID is collected for each increment by changing the ϕ_1 phase to $y,-y$. For States-TPPI acquisition, the ϕ_1 and ϕ_{rec} phases are also incremented by 180° every other ^{15}N increment. Gradients are Wurst shaped *z*-axis gradients with a length of 1 ms. Gradient strengths (G/cm): G1: 5, G2: 7, G3: 17. For the uniformly ^{15}N,^{13}C-labeled HscB and ubiquitin samples, in order to refocus $^{1}J_{NC^{\alpha}}$ coupling during the ^{15}N constant-time evolution, the CCLS-HSQC pulse sequence was modified as follows: for the 90° and 180° pulses on ^{13}C′, selective sinc shaped pulses were used with an excitation maximum at ^{13}C′ and a null at ^{13}C$^{\alpha}$, 113 ppm away; a selective squared 180° pulse with a maximum of excitation on ^{13}C$^{\alpha}$ was given at point *a* to decouple ^{15}N and ^{13}C$^{\alpha}$ nuclei during the constant-time evolution. In order to preserve water magnetization, our CCLS-HSQC pulse sequence is based on the fast HSQC experiment (Mori et al. 1995). According to this approach, water magnetization, which is placed on the transverse plane at the end of the first INEPT period, is dephased and rephased by the identical G2 gradients flanking the ^{15}N constant-time evolution period, and subsequently flipped back and preserved along the +Z axis for the reverse INEPT and acquisition periods. This is a very simple and robust experiment that works well for proteins

Materials and methods

This study made use of samples from three different proteins. The first protein we used was a uniformly doubly labeled sample of ubiquitin purchased from Martek Biosciences. The second protein was HscB from *Escherichia coli*, a 20 kDa J-type co-chaperone protein involved in iron sulfur cluster assembly. A sample of [U–^{13}C, U–^{15}N]-HscB produced from *E. coli* was generously provided by Dennis T. Ta and Larry E. Vickery (University of California, Irvine). The third protein was the 41-kDa C-subunit of mouse cAMP-dependent protein kinase A (PKA-C). We produced samples of PKA-C from *E. coli* cells, with two selective labeling patterns. Sample **A** was prepared by incorporating [^{13}C′]-Phe and [^{15}N]-Gly, and sample **B** was prepared by incorporating [^{13}C′]-Gly and [^{15}N]-Phe. PKA-C contains two Phe-Gly dipeptides (F54-G55, F185-G186), which should contain ^{13}C′–^{15}N linkages in sample **A**, and one Gly-Phe dipeptide (G186-F187), which should contain a ^{13}C′–^{15}N linkage in sample **B**.

NMR data were recorded on Varian VNMRS spectrometers equipped with a *z*-axis pulsed field gradient cold probe operating at ^{1}H Larmor frequencies of either 800 MHz (ubiquitin and PKA-C) or 600 MHz (HscB). Data for ubiquitin (1.5 mM, pH 6.5 in 50 mM phosphate buffer containing 7% D_2O) were acquired at 25 and 5°C, while data for HscB (1 mM, pH 7.4 in 20 mM Tris buffer containing 7% D_2O and 9 mM DTT) were acquired at 40, 30, 20, and 10°C, and data for PKA-C (0.3 mM, pH 6.5 in 20 mM phosphate buffer containing 10% D_2O, 180 mM KCl and 15 mM DTT) were acquired at 27°C.

2D CCLS-HSQC spectra were acquired on all protein samples using the pulse sequence shown in Fig. 1 and compared with spectra acquired with a ^{1}H–^{15}N 2D-version of a conventional HNCO sequence for ubiquitin and HscB (Ikura et al. 1990; Kay et al. 1990), and a TROSY HNCO experiment for PKA-C (Weigelt 1998). For the uniformly ^{15}N,^{13}C-labeled samples of HscB and ubiquitin, the CCLS-HSQC sequence shown in Fig. 1 was modified as described in the figure legend to refocus $^{1}J_{NC^{\alpha}}$ coupling during the ^{15}N constant-time evolution. For ubiquitin, all 2D CCLS-HSQC spectra were acquired with four scans and 64 complex points in the ^{15}N dimension, whereas eight transients were used for each FID of the 2D HN(CO) spectra. For HscB, all 2D data were acquired with 16 transients and 53 complex points in the ^{15}N dimension, except for spectra collected at the lowest temperature (10°C) for which 64 transients were accumulated for each FID. For the PKA-C samples, each 2D spectrum was collected using 640 scans and 40 complex points in the ^{15}N dimension. The software nmrPipe/nmrDraw (Delaglio et al. 1995) was used for data processing and initial visualization. Processing was achieved by zero filling to a final matrix size of 2048 × 128

points and applying a squared sine-bell window function shifted by 90° in both dimensions prior to Fourier transformation. Sparky software (Goddard and Kneller) was used for subsequent data visualization and for determining signal-to-noise (S/N) values.

The transverse relaxation rate, T_2, of the ^{15}N antiphase magnetization for ubiquitin and HscB was measured at various temperatures (*vide supra*) by recording a series of CCLS-HSQC reference spectra with increasing constant-time delays, $2T_{NC'}$, and fitting an exponential equation to the observed decaying signal. For HscB we collected 1D spectra, each accumulated with 1024 transients, and measured peak intensities by integrating over a region of the 1D ^{1}H spectra between 8.0 ppm and 9.4 ppm. For ubiquitin, instead, full 2D spectra were collected at various $T_{NC'}$ delays, allowing us to calculate the relaxation rate for each residue in the protein.

Description of the CCLS-HSQC pulse sequence

The CCLS-HSQC pulse sequence builds on the constant time (CT) HSQC experiment. Two spectra, a reference spectrum and a suppression spectrum, are acquired simultaneously in an interleaved manner. The reference spectrum is recorded using the pulse sequence shown in Fig. 1, with the 180° pulse on ^{13}C′ during the ^{15}N CT evolution period (open rectangle) applied at position *a*, simultaneous to the 180° ^{1}H pulse. This is essentially a CT HSQC experiment that yields a spectrum with decoupled ^{1}H–^{15}N signals. The suppression experiment is acquired with the 180° ^{13}C′ pulse at position *b*, simultaneous to the 180° ^{15}N pulse. This causes the ^{15}N–^{13}C′ coupling to be active during the CT period so as to convert the transverse magnetization of ^{15}N spins attached to ^{13}C′ ($2H_zN_x$ and $2H_zN_y$) into antiphase magnetization, $4H_zN_yC'_z$ and $4H_zN_xC'_z$, respectively. Neither of these terms will yield observable signal at the end of the sequence. The $4H_zN_xC'_z$ term, which is not affected by the ^{15}N 90° pulse given along the *x*-axis at the end of the ^{15}N evolution, is dephased by the G_2 gradient. The second term ($4H_zN_yC'_z$) is placed along the *z*-axis by the ^{15}N 90° pulse ($4H_zN_zC'_z$) and is not dephased by the G_2 gradient, but it is converted into unobservable multiple quantum coherence ($2H_xC'_y$) by the subsequent 90° pulses on ^{1}H and ^{13}C′, and the reverse INEPT period. As a consequence, signals from ^{1}H–^{15}N groups linked to ^{13}C′ are suppressed by this pulse scheme. On the other hand, magnetization from ^{12}C′-linked ^{1}H–^{15}N groups is unaffected by the suppression pulses on ^{13}C′ and results in cross-peaks that have the same intensity as in the reference spectrum. The suppressed spectrum could then be subtracted from the reference one, to cancel out ^{12}C′-linked resonances, leaving only the ^{13}C′-linked ^{1}H–^{15}N peaks. However, as explained in more detail below, this causes a loss in S/N for the CCLS method. An alternative and more advantageous strategy is not to subtract the data to obtain an edited spectrum, but rather to use the suppression spectrum only to identify which peaks in the reference spectrum are linked to ^{13}C′ nuclei.

A similar method was described earlier (Vuister et al. 1993) in which the difference in intensity between a reference and a suppression spectrum is used for accurately extracting the three-bond ^{15}N–^{13}C J couplings. Although technically similar, the intended purpose of the two experiments is quite different.

Signal-to-noise comparison between CCLS-HSQC and HNCO experiments

Signal from the CCLS-HSQC reference spectrum is regulated only by the exponential decay of the transverse ^{15}N antiphase magnetization during the constant-time period ($2T_{NC'}$), $\exp(-2T_{NC'}/T_2)$. In the CCLS-HSQC suppression experiment, on the other hand, the ^{15}N magnetization during the constant-time period is attenuated by the antiphase ^{15}N T_2 decay, $\exp(-2T_{NC'}/T_2)$, and modulated by the active $^1J_{NC'}$ coupling, $\cos(2\pi^1J_{NC'}T_{NC'})$. This additional cosine modulation will result in complete suppression of the ^{13}C′-linked ^{1}H–^{15}N peaks for the suppression spectrum when the constant-time delay is equal to $1/(2\ ^1J_{NC'})$, or $T_{NC'} = 1/(4^1J_{NC'})$.

If we subtract the suppression spectrum from the reference spectrum, the signal observed for the resulting edited spectrum is then given by the equation $[1 - \cos(2\pi^1 J_{NC'}T_{NC'})] \cdot \exp(-2T_{NC'}/T_2)$, which can also be written as $2 \cdot \sin^2(\pi^1J_{NC'}T_{NC'}) \cdot \exp(-2T_{NC'}/T_2)$. It can be easily shown from this formula that maximum signal will be obtained when the $T_{NC'}$ delay is set to $(1/\pi^1J_{NC'}) \cdot \mathrm{atan}(\pi^1J_{NC'}T_2)$. Surprisingly, this indicates that the maximum signal for the edited spectrum is obtained for constant-time periods that are longer than the $1/(2\ ^1J_{NC'})$ delay (or $T_{NC'} = 1/(4^1J_{NC'})$).

In a similar fashion, the signal resulting from an HNCO experiment is governed by the equation $\sin^2(2\pi^1J_{NC'}T_{NC'}) \cdot \exp(-4T_{NC'}/T_2)$, where $T_{NC'}$ is the time delay for half ^{15}N–^{13}C′ INEPT transfer and is repeated four times during the HNCO pulse sequence. To maximize signal for HNCO experiments, the $T_{NC'}$ delay will have to be set to $(1/2\ \pi^1J_{NC'}) \cdot \mathrm{atan}(\pi^1J_{NC'}T_2)$, i.e. at shorter values than for the edited CCLS-HSQC spectrum above.

In order to compare the S/N of the CCLS-HSQC and HNCO experiments, one must account for the fact that the CCLS-HSQC method requires the collection of two spectra; thus for the same data collection time, the number of scans accumulated in the HNCO experiment will be twice

the number of scans used in the reference and suppression CCLS-HSQC data accumulation. Furthermore, when the suppression CCLS-HSQC spectrum is subtracted from the reference, the noise in the resulting edited spectrum adds up to the same level as for the HNCO that was collected using twice as many scans. Hence, for a correct comparison of the CCLS-HSQC reference, subtraction and edited spectra with the HNCO, the formula describing their respective sensitivities must be multiplied by factors $\sqrt{2}$, $\sqrt{2}$, 1 and 2, respectively. The relative S/N curves for the HNCO and the CCLS-HSQC reference and edited spectra as a function of $T_{NC'}$ are shown in Fig. 2 for different values of T_2. It is clear that, when $T_{NC'}$ is optimized for each experiment to achieve maximum S/N, the CCLS-HSQC reference spectrum is the most sensitive, particularly for shorter $T_{NC'}$ values. This is even more remarkable if we consider that the CCLS-HSQC reference experiment is run for only half as long as the HNCO. On the other hand, due the increase in the noise level caused by the editing process, no gain in sensitivity is found for the CCLS-HSQC edited experiment over the HNCO.

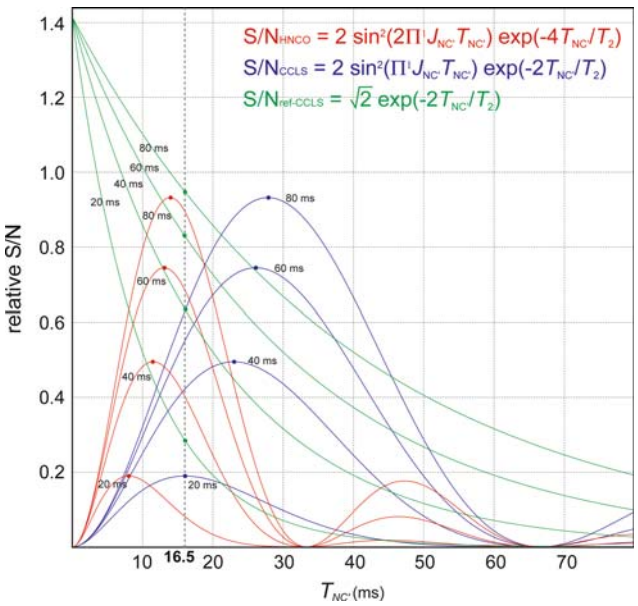

Fig. 2 Plot showing the relative signal-to-noise ratio, S/N, for the edited CCLS-HSQ, reference CCLS-HSQC and HNCO spectra as a function of the $T_{NC'}$ delay and for four different values of the ^{15}N antiphase transverse relaxation time constant, T_2. The $T_{NC'}$ delay used in the equations corresponds to half of the constant-time delay for the CCLS-HSQC experiments and to half of the ^{15}N–$^{13}C'$ INEPT transfers in the HNCO experiment. The colored dots on each curve indicate the maximum S/N obtainable for the edited CCLS-HSQC and HNCO experiments. For the reference CCLS-HSQC experiment, instead, the dots are set at the $T_{NC'}$ value that results in complete suppression of the ^{1}H–$^{15}N(-^{13}C')$ peaks in the suppression CCLS-HSQC spectrum. The equations that were used to calculate the curves are discussed in the Materials and Methods section and are also printed within the graph. This figure was generated using the commercially available program Grapher, version 1.0, from Apple Computer, Inc.

Thus, in order to take advantage of the CCLS-HSQC experiment's higher sensitivity, the best strategy is to use the suppression spectrum to identify which peaks in the reference spectrum belong to the ^{15}N–^{1}H groups attached to $^{13}C'$ nuclei, by comparing the peak intensities without subtracting the two spectra. Sensitivity is optimized by setting the CT delay to $1/(2^1J_{NC'})$, $T_{NC'} = 1/(4^1J_{NC'})$ (or possibly shorter for larger proteins with very short T_2) to achieve maximum reduction of the signals in the suppression spectrum, while retaining as much signal as possible in the reference spectrum. As described earlier, the signal for this spectrum is regulated only by the exponential decay of the transverse ^{15}N antiphase magnetization during the CT delay: $\exp(-2T_{NC'}/T_2)$. A careful analysis of the S/N curves for the various experiments (Fig. 2) reveals that for large proteins, with shorter T_2, the S/N yielded by the reference spectrum is higher than that of either the HNCO or CCLS-HSQC edited spectrum acquired at the optimal $T_{NC'}$ value. The advantage of the CCLS-HSQC reference spectrum over the HNCO experiment for larger proteins becomes even more evident when we plot the ratio between the S/N of the two experiments (reference CCLS-HSQC over HNCO) as a function of the antiphase ^{15}N T_2 decay rate. This relationship, calculated using the theoretical formulas discussed above, is shown in Fig. 3 along with our experimental results (see section below) and clearly demonstrates that the gain in sensitivity of the CCLS method over the HNCO steadily grows for proteins with ^{15}N T_2 values shorter than $\sim$85 ms. Another advantage of the CCLS-HSQC spectra over the HNCO is that, for larger proteins, the optimal $T_{NC'}$ value that yields maximum signal for HNCO becomes very short allowing only very few increments to be collected within the constant-time ^{15}N evolution.

Results and discussion

As an experimental verification of the theoretical equations describing the signal yielded by each experiment, we collected CCLS-HSQC reference and suppression spectra, as well as conventional HNCO spectra, for several different values of $T_{NC'}$, on a ubiquitin sample at two different temperatures: 5 and 25°C. The S/N for each cross-peak in the 2D spectra was measured and plotted against the $T_{NC'}$ delay, and the theoretical curves described above were fitted to the experimental points of the corresponding spectrum, by optimizing two parameters: the ^{15}N transverse relaxation time constant, T_2, and an arbitrary constant K. Figure 4 shows such a plot of measured S/N as a function of $T_{NC'}$ for a single residue, randomly chosen from

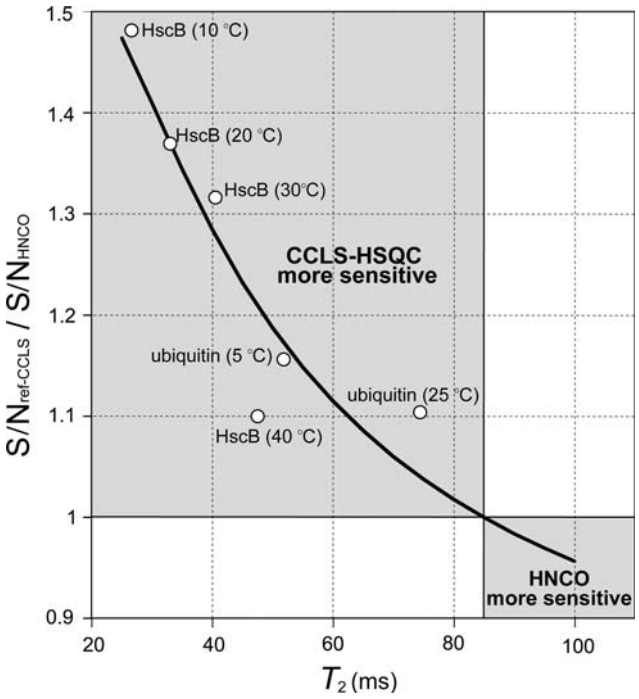

Fig. 3 Plot showing how the sensitivity gain of the CCLS-HSQC reference spectrum over the HNCO spectrum (given by the ratio between the S/N of the two experiments) changes as a function of the T_2 relaxation rate of the ^{15}N antiphase magnetization of the protein. The theoretical curve was calculated using the formulas described in the text using a $T_{NC'}$ delay of 16.5 ms for the CCLS-HSQC spectrum and using the optimized $T_{NC'}$ delay for any given T_2 value for the HNCO spectrum. The reported experimental points for ubiquitin were calculated by averaging the S/N ratios and the T_2 values calculated for each residue from 2D spectra. For HscB, the ^{15}N T_2 values were calculated by fitting the exponential decay of the signals comprised between 8.0 ppm and 9.5 ppm in a series of 1D CCLS-HSQC reference spectra acquired with increasing constant-time delays. The S/N ratios instead were calculated from 2D spectra as described in the text. This graph was made using KaleidaGraph

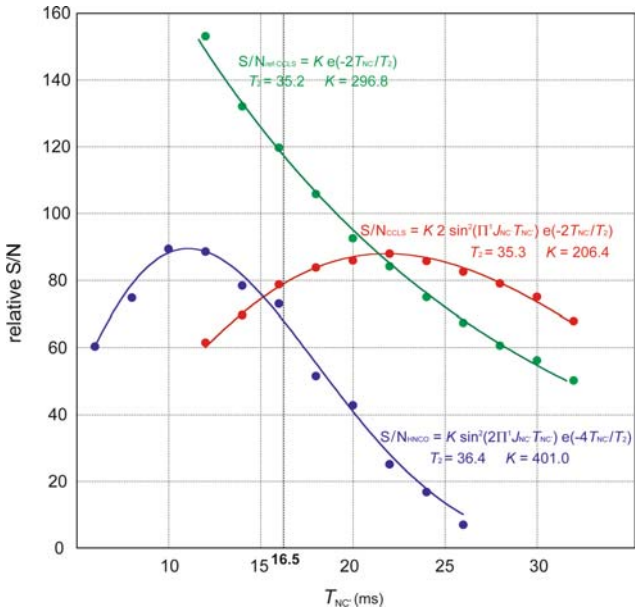

Fig. 4 Plot showing the S/N for the edited CCLS-HSQC, reference CCLS-HSQC and HNCO spectra measured at several different values of the $T_{NC'}$ delay for a single residue of ubiquitin (randomly chosen). 2D-^{1}H/^{15}N spectra were collected, processed and analyzed as described in the Materials and Methods section. The HNCO spectra were accumulated using twice as many scans as the reference or suppression CCLS-HSQC spectra. The edited CCLS-HSQC spectra were obtained by subtracting the suppression spectra from the corresponding reference ones. The equations giving the S/N for each spectrum were fitted to the experimental points by optimizing T_2 and K. It is interesting to note that the predicted value of K for the different spectra reflects the same 2:$\sqrt{2}$:1 ratio between the HNCO, reference CCLS-HSQC spectrum and edited CCLS-HSQC spectrum, respectively, as described in the text. The theoretical equations as well as the optimized values of T_2 and K are also shown in the plot. For this particular residue, curve fitting of the data from the three spectra yielded very similar values of ^{15}N T_2 ($\sim$35 ms). The ^{15}N T_2 value measured in this manner is the relaxation rate of the ^{15}N antiphase magnetization that is transverse during the constant-time period; it is this value of T_2 that plays a critical role in determining the signal intensities from the CCLS-HSQC and HNCO experiments. This plot and curve fitting were made using the commercially available program KaleidaGraph, version 3.6.2, by Synergy Software

the data set collected at 5°C as representative of the quality of the experimental data, and the curve fits achieved. For this particular residue, curve fitting of the experimental points for all three experiments yielded very similar values of ^{15}N T_2 ($\sim$35 ms). It is also interesting to note that the predicted value of K for the different spectra (HNCO spectrum, CCLS-HSQC reference spectrum and CCLS-HSQC edited spectrum) reflects the same 2:$\sqrt{2}$:1 ratio described above. Similar results were obtained for the other ubiquitin residues at 5 and 25°C.

As a test of the sensitivity of the CCLS method, we acquired reference CCLS-HSQC and conventional HNCO spectra on the 20-kDa [U–^{13}C, U–^{15}N]-HscB sample at 40, 30, 20, and 10°C, corresponding to average T_2 values of $\sim$47, 40, 33, and 27 ms. The signal-to-noise (S/N) ratio of each experiment decreased with lower temperature (Fig. 5), as expected from the increase in rotational correlation time of the protein in solution. Whereas the reference CCLS-HSQC sequence gave comparable signal to HNCO at 40°C, the reference CCLS-HSQC experiment became more sensitive than the HNCO as the temperature was lowered to simulate a larger protein. At 10°C, the conventional 2D-HN(CO) spectrum was quite poor, whereas the reference CCLS-HSQC spectrum still contained the majority of the cross peaks. At this temperature, the S/N ratios of reference CCLS-HSQC peaks were on average 50% higher than those of corresponding observable 2D-HN(CO) peaks (Table 1).

The average of the S/N ratio between the spectra (CCLS-HSQC reference over HNCO) measured for HscB and ubiquitin at the various temperatures was then plotted (Fig. 3) against the average of the corresponding antiphase

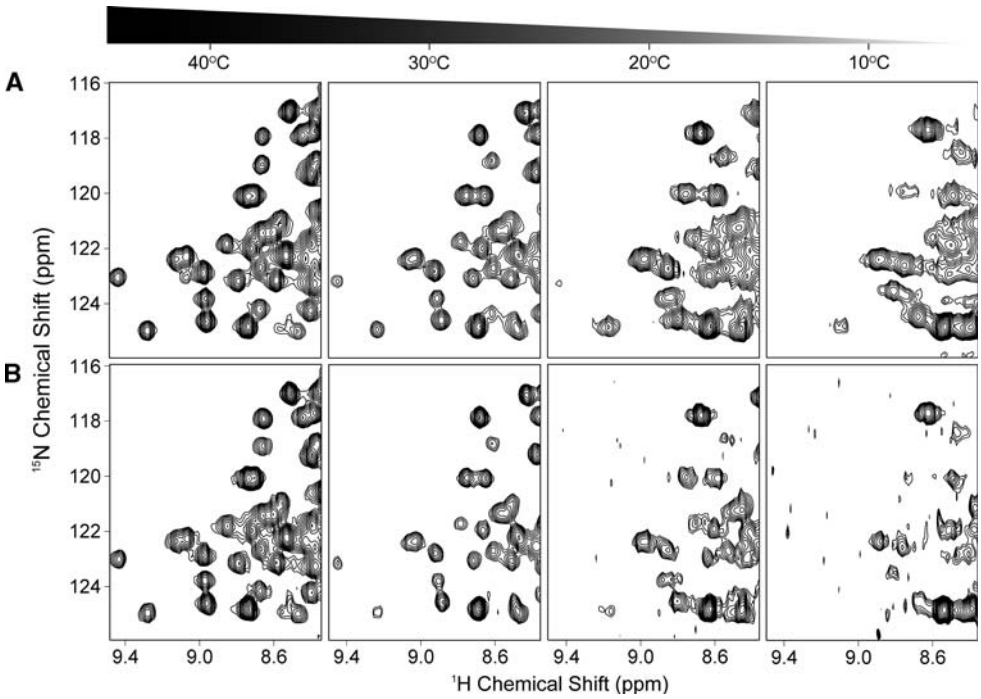

Fig. 5 2D-^{1}H/^{15}N spectra of the protein HscB taken at different temperatures using (**A**) the CCLS-HSQC pulse sequence and (**B**) the conventional 2D-HN(CO) pulse sequence. Identical acquisition parameters were used to collect the data using either sequence. Each FID was accumulated with 16 scans for all spectra, except for those run at 10°C, where 64 scans were used. All processing was performed identically for each data set

Table 1 NMR data for [U–^{13}C, U–^{15}N]-HscB acquired at various temperatures including the relative signal-to-noise ratios of cross peaks in the CCLS-HSQC and 2D-HN(CO) spectra

Temperature (°C)	40.0	30.0	20.0	10.0
T_2 (ms)[a]	47.5 ± 0.1	40.5 ± 0.3	33.0 ± 0.3	26.6 ± 0.6
Relative signal-to-noise: CCLS-HSQC/2D-HN(CO)[b]	1.10 ± 0.2	1.32 ± 0.3	1.37 ± 0.4	1.48 ± 0.5

[a] Relaxation times (T_2) were calculated as described in the Materials and Methods section

[b] The signal-to-noise ratio was the average for the observed CCLS-HSQC cross peaks divided by the average for the corresponding 2D-HN(CO) cross peaks. The S/N of the CCLS-HSQC reference spectra was scaled down by $\sqrt{2}$ to account for the fact that the CCLS-HSQC and HNCO spectra were collected using the same number of transients

^{15}N T_2 rates. The experimental data points follow the same trend as the theoretical curve, calculated using the equations described earlier, clearly demonstrating that the CCLS approach is superior to the conventional 2D-HN(CO) experiment, with a significant sensitivity gain for large proteins.

We then applied the CCLS-HSQC method to the 41-kDa catalytic subunit of cAMP-dependent protein kinase A (PKA-C). PKA-C catalyzes the transfer of the γ-phosphate from ATP to a hydroxyl group of a serine or threonine residue. It is the most highly conserved member of the Ser/Thr kinase family and has therefore served as the prototype for this family of enzymes (Taylor et al. 2005). Protein kinases are involved in a number of signal transduction cascades, including cell growth, proliferation, and death, making them ideal candidates as a target for drug design (Taylor et al. 2005). This family of enzymes has remained relatively unexplored by NMR because of undesirable spectral characteristics related to the size of its members and the presence of conformational exchange effects on the µs-ms timescale (Langer et al. 2004, 2005; Vogtherr et al. 2005, 2006). Previous efforts to assign the resonances of PKA-C by TROSY-based 3D experiments yielded assignments to only ~55% of the non-proline residues (Langer et al. 2004). Among the missing assignments were highly conserved dynamic residues located in loops and turns in the active site of the enzyme directly involved in the catalytic cycle (Taylor et al. 2004, 2005): Specifically, residues within the glycine-rich loop and the DFG-motif central to enzyme function. Our own attempts to assign these residues (data not shown) either by 3D experiments on perdeuterated enzyme or by incorporating pairs of ^{15}N- and ^{13}C′-labeled amino acids with detection by 2D-[^{1}H/^{15}N]-TROSY-HN(CO) were unsuccessful.

The CCLS-HSQC reference spectrum for sample **A** (Fig. 6A) revealed 29 resonances. Because the primary sequence of PKA-C contains 22 glycines, the additional signals arose from scrambling of the label from [^{15}N]-Gly. Biosynthetic exchange of labels between Gly and Ser is common in recombinant proteins produced from *E. coli*

(Lian and Middleton 2001). Nevertheless, the suppression spectrum showed reduction in the intensity of resonances only from glycines linked to $^{13}C'$-Phe. Only two peaks were identified by the suppression spectrum, one of which (G55) could be assigned based on 3D spectra; while the remaining resonance which does not have correlations in the 3D data sets was assigned to G186.

PKA-C contains only one Gly-Phe dipeptide, corresponding to G186 and F187. For sample **B**, the CCLS-HSQC reference spectrum (Fig. 6B) contained signals only from the 25 Phe residues in the PKA-C primary sequence, and hence showed no evidence for isotope scrambling. However, as demonstrated for sample **A**, the isotopic enrichment of $^{13}C'$-Gly was diluted by biosynthetic exchange. Therefore, the F187 resonance intensity was reduced, rather than canceled, in the suppression CCLS-HSQC experiment. By comparing the reference and suppression CCLS-HSQC spectra, only one cross peak was identified which was then unambiguously assigned to F187. Assignments made in this manner have enabled us to map the chemical shift effects of nucleotide and substrate binding in the DFG-motif (Masterson et al. (submitted)).

Conclusions

We present here a highly sensitive pulse sequence (CCLS-HSQC) for the detection of signals from ^{1}H–^{15}N units involved in a $^{13}C'$–^{15}N linkage. A careful analysis of the formulas that govern the amount of signal obtained by the CCLS-HSQC and HNCO experiments indicates that the CCLS-HSQC pulse sequence provides higher sensitivity for larger proteins than the conventional HNCO. The difference becomes more obvious when the sensitivity gain provided by the CCLS-HSQC method over the conventional HNCO experiment is plotted as a function of the ^{15}N T_2 of the protein (Fig. 3); the ratio of the S/N between the two spectra clearly favors the CCLS-HSQC experiment for ^{15}N T_2 values shorter than $\sim$85 ms, with bigger gains achieved for larger proteins with shorter ^{15}N T_2.

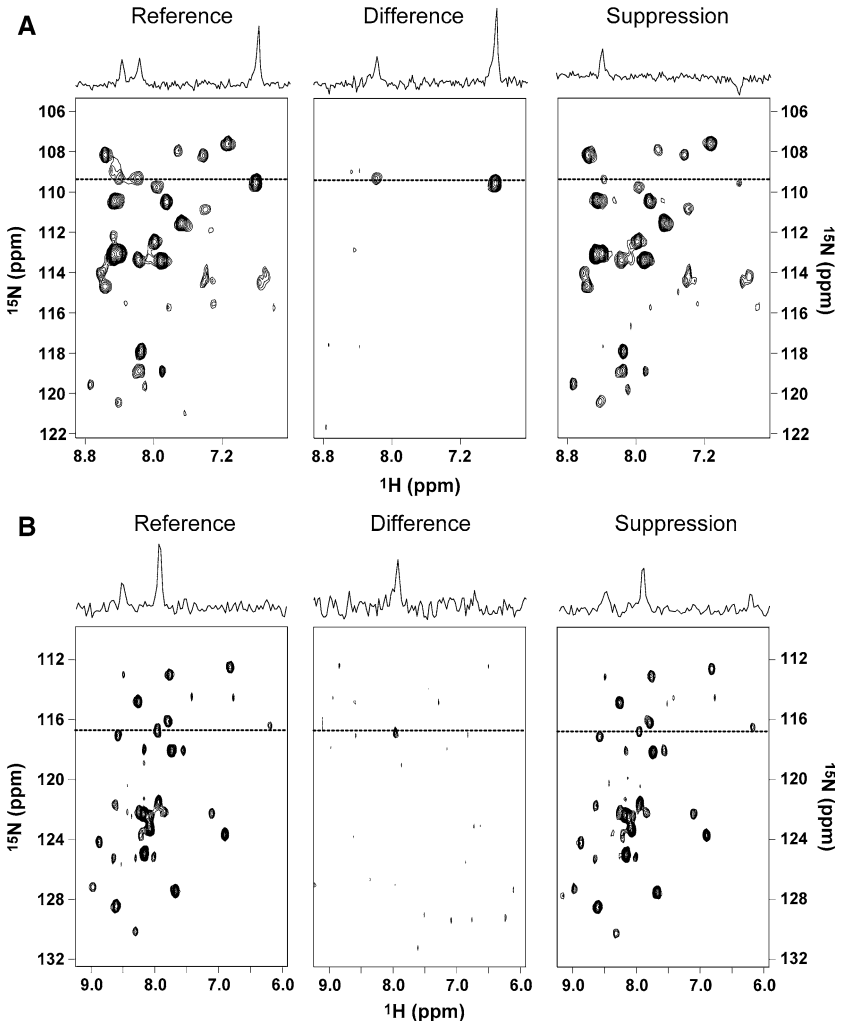

Fig. 6 Spectra of the 41-kDa enzyme PKA-C utilizing the CCLS-HSQC sequence. (**A**) Sample **A** containing ^{15}N-Gly combined with $^{13}C'$-Phe produced more than the expected resonances in the HSQC due to scrambling, but only 2 of the resonances expected peaks in the CCLS-HSQC. (**B**) Sample **B** containing ^{15}N-Phe combined with $^{13}C'$-Gly produced 25 of the expected resonances in the HSQC spectrum and one of the expected resonances in CCLS-HSQC

As a verification of the sensitivity of the method, we acquired several 2D CCLS-HSQC and HNCO spectra at various temperatures on ubiquitin and a 20-kDa-protein sample. As shown in Fig. 4, the experimental data we obtained is in good agreement with our theoretical considerations, further proving that the CCLS-HSQC experiment is more sensitive than HNCO for larger proteins. We then used the CCLS-HSQC experiment on selectively labeled PKA-C samples to assign a critical residue in a case where conventional 2D-HN(CO) had failed (Masterson et al. (submitted)). Although the approach requires that the ^{1}H–^{15}N HSQC cross peaks be observable, it does not require deuteration of the protein. The method is suitable for larger proteins and is less affected by conformational exchange than HNCO experiments, which require a longer period of transverse ^{15}N magnetization. The method also is tolerant to the partial loss of signal from isotopic dilution (scrambling). Finally, CCLS-HSQC can be used with combinatorial selective labeling schemes (Parker et al. 2004) and algorithms that provide optimized choices for potential assignments from $^{15}N/^{13}C'$ labeling (Trbovic et al. 2005). This approach will allow NMR investigations of families of proteins that have hitherto been resistant to NMR structural and dynamic analysis, such as large enzymes and unfolded proteins.

Acknowledgements We thank Professor Susan S. Taylor for generously supplying the plasmid for PKA-C and Dr. Alessandro Mascioni for assistance with NMR sample preparation. We thank Dennis T. Ta, Anna K. Füzery, and Prof. Larry E. Vickery for graciously lending the HscB sample. This work was supported by NIH Grants RR02301 and GM66326 (Markley, J.L.), GM64742, GM072701 (Veglia, G.) and American Heart Association support from 0615546Z (Masterson, L.R.).

References

Abdulaev NG, Ngo T, Ramon E, Brabazon DM, Marino JP, Ridge KD (2006) The Receptor-Bound "Empty Pocket" State of the Heterotrimeric G-Protein α-Subunit Is Conformationally Dynamic. Biochemistry 45:12986–12997

Clore GM, Gronenborn AM (1994) Multidimensional heteronuclear nuclear magnetic resonance of proteins. Meth Enzymol 239:349–363

Delaglio F, Grzesiek S, Vuister GW, Zhu G, Pfeifer J, Bax A (1995) NMRPipe: a multidimensional spectral processing system based on UNIX pipes. J Biomol NMR 6:277–293

Gardner KH, Zhang X, Gehring K, Kay LE (1998) Solution NMR Studies of a 42 kDa *Escherichia coli* Maltose Binding Protein/beta-Cyclodextrin Complex: Chemical Shift Assignments and analysis. J Am Chem Soc 120:11738–11748

Goddard TD, Kneller DG, SPARKY 3, University of California, San Francisco

Ikura M, Kay LE, Bax A (1990) A novel approach for sequential assignment of ^{1}H, ^{13}C, and ^{15}N spectra of proteins: heteronuclear triple-resonance three-dimensional NMR spectroscopy. Application to calmodulin. Biochemistry 29:4569–4667

Kainosho M, Tsuji T (1982) Assignment of the three methionyl carbonyl carbon resonances in Streptomyces subtilisin inhibitor by a carbon-13 and nitrogen-15 double-labeling technique. A new strategy for structural studies of proteins in solution. Biochemistry 21:6273–6279

Kay LE, Ikura M, Tschudin R, Bax A (1990) Three-dimensional triple-resonance NMR spectroscopy of isotopically enriched protein. J Magn Reson 89:496–514

Langer T, Sreeramulu S, Vogtherr M, Elshorst B, Betz M, Schieborr U, Saxena K, Schwalbe H (2005) Folding and activity of cAMP-dependent protein kinase mutants. FEBS Lett 579:4049–4054

Langer T, Vogtherr M, Elshorst B, Betz M, Schieborr U, Saxena K, Schwalbe H (2004) NMR backbone assignment of a protein kinase catalytic domain by a combination of several approaches: application to the catalytic subunit of cAMP-dependent protein kinase. Chembiochem 5:1508–1516

Lian LY, Middleton DA (2001) Labelling approaches for protein structural studies by solution-state and solid-state NMR. Progress in Nuclear Magnetic Resonance Spectroscopy 39:171–267

McIntosh LP, Dahlquist FW (1990) Biosynthetic incorporation of ^{15}N and ^{13}C for assignment and interpretation of nuclear magnetic resonance spectra of proteins. Q Rev Biophys 23:1–38

Mori S, Chitrananda A, O'Neil Johnson M, van Zijl PCM (1995) Improved sensitivity of HSQC spectra of exchanging protons at short interscan delays using a new fast HSQC (FHSQC) detection scheme that avoids water saturation. J Magn Reson B 108:94–98

Parker MJ, Aulton-Jones M, Hounslow AM, Craven CJ (2004) A combinatorial selective labeling method for the assignment of backbone amide NMR resonances. J Am Chem Soc 126: 5020–5021

Pervushin K, Riek R, Wider G, Wüthrich K (1997) Attenuated T_2 relaxation by mutual cancellation of dipole-dipole coupling and chemical shift anisotropy indicates an avenue to NMR structures of very large biological macromolecules in solution. Proc Natl Acad Sci USA 94:12366–12371

Riek R, Fiaux J, Bertelsen EB, Horwich AL, Wüthrich K (2002) Solution NMR techniques for large molecular and supramolecular structures. J Am Chem Soc 124:12144–12153

Taylor SS, Kim C, Vigil D, Haste NM, Yang J, Wu J, Anand GS (2005) Dynamics of signaling by PKA. Biochim Biophys Acta 1754:25–37

Taylor SS, Yang J, Wu J, Haste NM, Radzio-Andzelm E, Anand G (2004) PKA: a portrait of protein kinase dynamics. Biochim Biophys Acta 1697:259–269

Trbovic N, Klammt C, Koglin A, Lohr F, Bernhard F, Dötsch V (2005) Efficient strategy for the rapid backbone assignment of membrane proteins. J Am Chem Soc 127:13504–13505

Tugarinov V, Hwang PM, Kay LE (2004) Nuclear magnetic resonance spectroscopy of high-molecular-weight proteins. Annu Rev Biochem 73:107–146

Tzakos AG, Grace CR, Lukavsky PJ, Riek R (2006) NMR techniques for very large proteins and rnas in solution. Annu Rev Biophys Biomol Struct 35:319–342

Vogtherr M, Saxena K, Hoelder S, Grimme S, Betz M, Schieborr U, Pescatore B, Robin M, Delarbre L, Langer T, Wendt KU, Schwalbe H (2006) NMR characterization of kinase p38 dynamics in free and ligand-bound forms. Angew Chem Int Ed Engl 45:993–997

Vogtherr M, Saxena K, Grimme S, Betz M, Schieborr U, Pescatore B, Langer T, Schwalbe H (2005) NMR backbone assignment of the mitogen-activated protein (MAP) kinase p38. J Biomol NMR 32:175

Vuister GW, Wang AC, Bax A (1993) Measurement of three-bond nitrogen-carbon J couplings in proteins uniformly enriched in ^{15}N and ^{13}C. J Am Chem Soc 115:5334–5335

Wagner G (1993) Prospects for NMR of large proteins. J Biomol NMR 3:375–385

Weigelt J (1998) Single scan, sensitivity- and gradient-enhanced TROSY for multidimensional NMR experiments. J Am Chem Soc 120:10778–10779

Yabuki T, Kigawa T, Dohmae N, Takio K, Terada T, Ito Y, Laue ED, Cooper JA, Kainosho M, Yokoyama S (1998) Dual amino acid-selective and site-directed stable-isotope labeling of the human c-Ha-Ras protein by cell-free synthesis. J Biomol NMR 11: 295–306